


# Continuous Hydrogenolysis of *N*-Diphenylmethyl Groups in a Micropacked-Bed Reactor

Jiacheng Tu,<sup>†,‡</sup> Le Sang,<sup>†</sup> Han Cheng,<sup>†</sup> Ning Ai,<sup>‡</sup> and Jisong Zhang<sup>\*,†</sup> 

<sup>†</sup>State Key Laboratory of Chemical Engineering, Department of Chemical Engineering, Tsinghua University, Beijing 100084, China

<sup>‡</sup>School of Chemical Engineering, Zhejiang University of Technology, Hangzhou 310014, Zhejiang, China

## Supporting Information

**ABSTRACT:** In recent years, with the advancements in continuous flow technology and the ever-increasing demand for green processes, continuous flow chemistry has become more and more widely adopted in the pharmaceutical industry. In this work, the continuous hydrogenolysis of *N*-diphenylmethylazetid-3-ol to 3-azetid-3-ol in micropacked bed reactors was demonstrated. The effects of different catalysts, solvent types, and the additives on the reaction in a micropacked-bed reactor were investigated. The results indicate that the reaction rate per reactor volume is increased by 100 times because of the larger interfacial area and shorter diffusion distance in micropacked reactors. To further study the long-term stability of the reaction system, the flow system was successfully operated for 240 h by adjusting the reaction temperature and liquid flow rate. The reaction kinetics model for the hydrogenation of *N*-diphenylmethylazetid-3-ol in methanol was studied after the internal and external diffusion limitations were eliminated. In addition, the type of adsorption of the reactants on the catalyst and the rate-determining step of the reaction were investigated.

**KEYWORDS:** hydrogenation, debenzilation, kinetics, micro-packed bed reactors

## INTRODUCTION

The hydrogenation reactions are ubiquitous chemical transformations in petrochemical industry, food industry, and pharmaceutical industry. About 9% of all chemical transformations in the pharmaceutical synthesis are hydrogenation reactions.<sup>1</sup> In addition to the common hydrogenations of unsaturated bonds, deprotection reactions with H<sub>2</sub> (hydrogenolysis) are also widely used in organic synthesis, accounting for about 3% of total pharmaceutical synthesis.<sup>1</sup>

In the production of pharmaceuticals and fine chemicals, protection and deprotection of functional groups such as alcohols and amines are often necessary to avoid possible side reactions.<sup>2</sup> In particular, formation and cleavage of benzyl-type ethers and benzyl-type amines represent a common strategy in organic synthesis.<sup>3</sup> The benzyl group is easily installed, by substitution of benzyl halide<sup>4</sup> or condensation of benzaldehyde,<sup>5</sup> and is stable to mild aqueous acid/base solutions, metal hydrides, and mild oxidants.<sup>3a</sup> Later, it can be removed through direct hydrogenation with the gas of H<sub>2</sub>, transfer hydrogenation with NaBH<sub>4</sub>, or using Lewis acids such as AlCl<sub>3</sub> or triflic acid.<sup>6</sup> Among these methods, precious metal-catalyzed hydrogenolysis with high pressure gas of H<sub>2</sub> is one of the green and efficient options, in accordance with “atom economy”, “reduce derivative”, and “catalysis” described in the green chemistry principles.<sup>7</sup>

The batch reactor is widely used for hydrogenation in the pharmaceutical industry and fine chemical industry because the reactor structure is simple. However, there are still several problems limiting its application. First, the heterogeneous hydrogenation is usually thought to be a fast reaction.<sup>8</sup> Because of the severe gas–liquid mass transfer limitation for hydrogenation in batch reactors, a long reaction time (3–24 h) and a large reactor volume (1000–5000 L) are required in the

industry production. Second, multiple gas replacement operations and separation of the catalysts are needed for one batch production, which is troublesome and labor-intensive. Third, there is a safety issue for the hydrogenation process because of the storage of a great amount of pressurized hydrogen and frequent operation of a palladium carbon catalyst.<sup>9</sup> As a result, it is highly desired to develop a safe and efficient hydrogenation method for pharmaceutical industry and fine chemical industry.

The continuous flow technology has been identified as the number one research area for the advancement of green pharmaceuticals by the ACS GCI Pharmaceutical Roundtable.<sup>10</sup> Continuous flow processes have many inherent advantages including the effective suppression of side reactions by precise control of reaction conditions, reduced cost of the separation/purification process, increased production, reduced energy consumption, reduced equipment volume, and excellent safety.<sup>11</sup> Among them, the continuous hydrogenation in micropacked-bed reactors ( $\mu$ PBRs) is promising for the challenges of hydrogenation. In  $\mu$ PBRs, the pressurized hydrogen and liquid reactants flow concurrently through packed beds of catalyst particles with diameters usually smaller than 500  $\mu$ m. Because of the microscale dimension, it has the advantages of good gas–liquid–solid mass transfer, excellent heat transfer and improved safety while maintaining the plug flow characteristics and fixed-bed catalyst immobilization.<sup>12</sup> Desai et al. achieved the selective debenzilation of the substrate containing acylamide and a carbon–carbon double-bond structure in the H-cube packed-bed reactors.<sup>13</sup> This reaction was performed with Pd/C catalysts under 1 bar, 40 °C

**Received:** September 26, 2019

**Published:** December 4, 2019

and a low liquid rate of 1.0 mL/min with the yield of 95%. Matos et al. successfully achieved simultaneous removal of multiple benzyl groups in  $\mu$ PBRs with a yield of 89% under 80 bar and 60 °C with Pd/C catalysts.<sup>14</sup> These results demonstrate the efficiency and safety of  $\mu$ PBRs in debenzilation than that of the batch reactor.

In this paper, a flow system based on  $\mu$ PBRs was developed to perform the H<sub>2</sub>-based hydrogenolysis. The hydrogenolysis of *N*-diphenylmethazetidin-3-ol (DMAOL) to 3-azetidinol (Figure 1) was employed as the model reaction, which is an

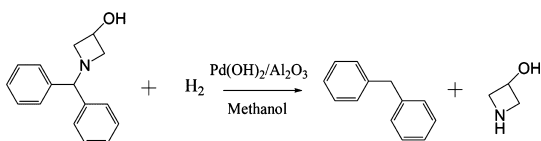


**Figure 1.** Hydrogenolysis of *N*-diphenylmethazetidin-3-ol to 3-azetidinol.

organic pharmaceutical intermediate for the synthesis of antibiotics and antibacterial agents.<sup>15</sup> The catalysts and solvents suitable for this kind of reaction were first screened and then the reaction performance and kinetics were investigated.

## MATERIAL AND METHODS

**Chemicals.** *N*-Diphenylmethazetidin-3-ol (C<sub>16</sub>H<sub>17</sub>NO) was acquired from PharmaBlock Sciences Ltd. (Nanjing); methanol (CH<sub>3</sub>OH, 99.9%) and acetonitrile (C<sub>2</sub>H<sub>3</sub>N, 99.9%) were purchased from J&K Scientific Ltd. (Beijing); tetrahydrofuran (C<sub>4</sub>H<sub>8</sub>O, AR), ethyl acetate (C<sub>4</sub>H<sub>8</sub>O<sub>2</sub>, AR), toluene (C<sub>7</sub>H<sub>8</sub>, AR), and triethylamine (C<sub>6</sub>H<sub>15</sub>N, AR) were purchased from Beijing Tongguang Fine Chemicals Company; 2-methyltetrahydrofuran (C<sub>5</sub>H<sub>10</sub>O, 99%) was purchased from Energy Chemical; diphenylmethane (C<sub>13</sub>H<sub>12</sub>, 99%) was purchased from Nuobeiwei Technology Co. Ltd. (Beijing); and acetic acid (CH<sub>3</sub>COOH, 99.5%) was purchased from Beijing Chemical Factory. Hydrogen (H<sub>2</sub>, 99.999%) was purchased from Beijing Beiweng Gas Manufacturing Plant. Nitrogen (N<sub>2</sub>) was purchased from Air Liquide (Tianjin). The palladium hydroxide/alumina particle catalyst (Pd(OH)<sub>2</sub>/Al<sub>2</sub>O<sub>3</sub>, 7 wt %) with an average size of 500  $\mu$ m and the palladium/alumina particle catalyst (Pd/Al<sub>2</sub>O<sub>3</sub>, 5 wt %) with an average size of 500  $\mu$ m were acquired from Dalian Institute of Chemical Physics. The palladium/carbon powder catalyst (Pd/C, 5 wt %, 55% water content) and the palladium hydroxide/carbon powder catalyst (Pd/(OH)<sub>2</sub>/C, 5 wt %, 55% water content) were acquired from HEOWNS Biochem Technology LLC (Tianjin) and Macklin Biochemical Co. Ltd. (Shanghai), respectively.

**Experimental Setup.** A schematic overview of the experimental setup is shown in Figure 2. Liquid was delivered by a plunger pump (Beijing Oushisheng Technology Co. Ltd.). N<sub>2</sub> gas and H<sub>2</sub> gas from the regulated cylinder were fed via a mass flow controller (Beijing Sevenstar Electronics Co. Ltd.); the outlet of the pump was connected with a safety valve (Beijing Xiongchuan Technology Co. Ltd.) to automatically release the liquids from the tubing when the pressure exceeded 40 bar. Two pressure gauges were placed in the inlet and outlet of the reactor to monitor the pressure drop across the reactor. The reactor and two coils were immersed in a water bath to control the reaction temperature. The outlet of the packed bed

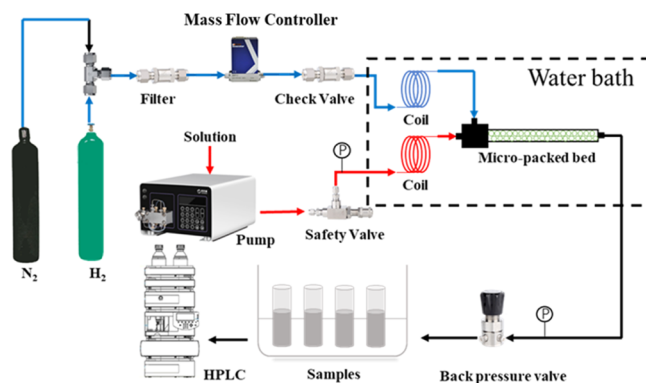


**Figure 2.** Schematic overview of the flow system for hydrogenation based on the  $\mu$ PBRs.

was connected to a back pressure regulator (Beijing Xiongchuan Technology Co. Ltd.) to control the system pressure.

The mixing of the feeding gas and liquid before the entering the packed-bed reactor greatly affects the stability and reproducibility of the system. To minimize the hydrodynamic instabilities, the reactor structure followed the design which was described in the literature<sup>16</sup> and more details about the reactor structure can be found in this paper. The packed tube is made of stainless steel with a length of 20 cm, an outer diameter of 6.35 mm (1/4 in.), and an inner diameter of 4.35 mm.

The reactant DMAOL was prepared as a specific concentration in the solvent. The particulate catalysts were filled into the reactor through a funnel and the catalyst bed was packed as tight as possible. The micropacked bed packed with a certain mass of the catalyst was pretreated by the solution, and then H<sub>2</sub> was transported into the reactor at a specific flow rate ( $F_G$ ). The Back pressure ( $P$ ) and the liquid flow rate ( $F_L$ ) were then set to the required values while simultaneously raising the system temperature ( $T$ ). After waiting for the reaction time, which was at least three times of the liquid residence time ( $\tau$ ), the system achieved a steady state and a sample was collected. When the desired samples were acquired, the water bath was turned off and the system pressure was reduced to atmospheric pressure. After the system was depressurized, N<sub>2</sub> gas was transported through the micropacked-bed reactor to fully remove the residual gas–liquid mixture and ensure that the catalyst was stored in a nitrogen atmosphere.

As hydrogenation in  $\mu$ PBRs involves the gas–liquid–solid process, the residence time of liquid  $\tau$  representing the reaction time should be carefully calculated. According to the definition of liquid holdup in our previous paper,<sup>16</sup>  $\tau$  is calculated by the following equation

$$\tau = \frac{\pi D^2 L \varepsilon h}{F_L} \quad (1)$$

where,  $D$  (cm) and  $L$  (cm) are the inner diameter and the length of the packed tubing, respectively;  $\varepsilon$  is the bed porosity; and  $h$  is the liquid holdup representing the fraction of interstitial open space filled by liquid. From this equation, we can find that the residence time is only determined by the liquid holdup, which can be calculated with the equations reported in the literature.<sup>16</sup>

Table 1. Comparison of the Catalytic Activities of Several Catalysts on the Hydrogenolysis of DMAOL<sup>a</sup>

catalyst	conversion (%)	catalyst activity [ $\text{g}(\text{raw material}) \times \text{g}(\text{catalyst})^{-1} \times \text{min}^{-1}$ ]
Pd/C (5 wt %, 55% H <sub>2</sub> O content)	36.9	0.31
Pd/Al <sub>2</sub> O <sub>3</sub> (5 wt %)	28.3	0.11
Pd(OH) <sub>2</sub> /C (5 wt %, 55% H <sub>2</sub> O content)	86.3	0.73
Pd(OH) <sub>2</sub> /Al <sub>2</sub> O <sub>3</sub> (7 wt %)	86.4	0.23

<sup>a</sup>Experimental conditions: flow rate of DMAOL (3.8 wt % in methanol) solution: 0.3 mL/min;  $P = 21$  bar;  $T = 313.15$  K;  $F_G = 40$  sccm (the molar ratio of H<sub>2</sub> to DMAOL: 43); and the amount of the catalyst (diluted with 4.5 g alumina sphere): 0.5 g.

**Sample Analysis.** The samples were collected directly from the outlet of the hydrogenation system. The samples were diluted and measured by HPLC (Agilent 1260 Infinity II) with a UV detector under the following conditions: the column temperature, 30 °C; the injection volume, 5  $\mu\text{L}$ ; the ultraviolet wavelength, 220 nm; the mobile phase composition, acetonitrile/water (70:30, v/v), 1.0 mL/min; and the column, Agilent Eclipse plus C18 (4.6  $\times$  250 mm, 5  $\mu\text{m}$ ). No side reaction was observed when performing hydrogenolysis of DMAOL in the  $\mu\text{PBRs}$ . Hence, the selectivity of the reaction is assumed to be 100%. The product of 3-zaetidinol cannot be measured by HPLC because it has no UV absorption. Only the concentrations of DMAOL and diphenylmethane are measured to calculate the conversion ( $X$ ) of DMAOL as follows.

$$X = \frac{C_B}{C_A + C_B} \times 100\% \quad (2)$$

where,  $C_A$  (mol/L) and  $C_B$  (mol/L) are the concentration of DMAOL and diphenylmethane in the sample, respectively.

## RESULTS AND DISCUSSION

**Screening Reaction Conditions.** As we know that the catalyst and solvent have a great influence on the hydrogenation. To develop a most efficient continuous hydrogenolysis in  $\mu\text{PBRs}$ , the screening of the catalyst and solvent was first performed.

**Effect of Catalyst.** It is well known that catalytic activity can be influenced by the catalyst type and support. It has been reported that Pd on activated carbon is more effective for debenzylation than Pd on oxide supports such as SiO<sub>2</sub>, Al<sub>2</sub>O<sub>3</sub>, and TiO<sub>2</sub>.<sup>17</sup> In addition, Pearlman's catalyst—Pd(OH)<sub>2</sub>/C<sup>18</sup> was commonly used in the debenzylation reaction, which demonstrated the best catalytic activity.<sup>19</sup> In this study, the catalysts of Pd and Pd(OH)<sub>2</sub> on the supports of activated carbon and alumina were tested under the same conditions. The reaction performances and the catalytic activities using different catalysts are given in Table 1. Here the mass of the substrate converted per unit time and unit mass catalyst [ $\text{g}(\text{raw material}) \times \text{g}(\text{catalyst})^{-1} \times \text{min}^{-1}$ ] was used to evaluate the catalyst activity.

From Table 1, it can be concluded that the catalytic activity of the Pd(OH)<sub>2</sub> catalyst is about two times that of the Pd catalyst for the hydrogenolysis reaction. At the same time, it also proves that the Pd or Pd(OH)<sub>2</sub> catalyst on activated carbon is more efficient than Pd or Pd(OH)<sub>2</sub> on oxide supports of Al<sub>2</sub>O<sub>3</sub>. However, the carbon support used here was at a powder state, which would cause a large pressure drop and even clogging in  $\mu\text{PBRs}$ . For the oxide supports of Al<sub>2</sub>O<sub>3</sub>, no significant pressure drop was observed, which means that values of the pressure transducers before and after the packed-bed reactor were almost the same. As a result, the Pd(OH)<sub>2</sub>/Al<sub>2</sub>O<sub>3</sub> catalyst was adopted for the following research in this paper.

**Effect of Solvent.** In hydrogenation, the solvent frequently plays an important role,<sup>20</sup> which would affect the solubility of hydrogen, adsorption mechanism of solvent molecules on the active sites of the catalyst, agglomeration of catalyst particles, and nonbonding interactions between the reactant or product molecules with the solvent.<sup>21</sup> The choice of a suitable solvent can effectively increase the reaction rate, and conversely, it will inhibit the reaction rate and even poison the catalyst. Here, the effect of some common organic solvents was explored. To ensure that the catalyst has the same catalytic activity, the reaction using the solvent of methanol was performed for a catalyst activity test every time before the solvents were changed.

Figure 3 shows the effect of several organic solvents on the conversion of DMAOL at the same experimental conditions.

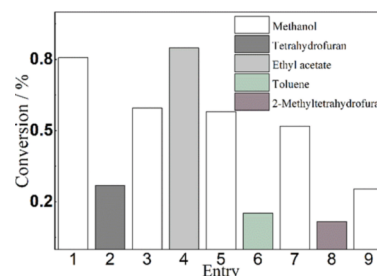


Figure 3. Conversion of DMAOL in different solvents. Experimental conditions: flow rate of DMAOL (3.8 wt % in methanol) solution: 0.5 mL/min;  $P = 21$  bar;  $T = 313.15$  K;  $F_G = 40$  sccm (the molar ratio of H<sub>2</sub> to DMAOL: 26); and the amount of the 7 wt % Pd(OH)<sub>2</sub>/Al<sub>2</sub>O<sub>3</sub> catalyst (diluted with 4.0 g alumina sphere): 1.0 g.

When the solvents are methanol and ethyl acetate,  $X$  can reach about 81 and 85% at a residence time of 2.1 min in the micropacked bed, indicating the beneficial effect on the catalytic activity. Compared with the two solvents, the reaction rates in the other three solvents are much slower. In addition, it is found that the  $X$  is abruptly decreased after the use of tetrahydrofuran (entry 2) and 2-methyltetrahydrofuran (entry 8). It indicates that tetrahydrofuran substances have a certain toxic effect on the catalyst which should be avoided in the reaction. However, the reason for this toxic effect is still unclear and we did not find any reports about the toxic effect of tetrahydrofuran for the hydrogenolysis with Pd(OH)<sub>2</sub> catalysts. Further research are required to find the exact mechanism of catalyst deactivation. As a result, both methanol and ethyl acetate are excellent solvents for hydrogenation of DMAOL. Considering the low price and easy recyclability of methanol (low boiling point), methanol is chosen as the solvent for this reaction.

**Effect of Additive.** It is known that *N*-benzyl is the acid-labile protecting group. Acidic conditions favor *N*-debenzylation, while basic conditions inhibit *N*-debenzylation.<sup>22</sup> In order



to investigate whether the effect of acidic or basic additives on the removal of the diphenylmethyl group was similar to that of debenzylation, an experiment was carried out by adding acetic acid and triethylamine to the solution. The conversions with different additives are given in Table 2.

**Table 2. Effect of the Additive on Conversion of DMAOL<sup>a</sup>**

entry	pressure/bar	additive	conversion/%
1	21	no additive	79.7
2	21	acetic acid	91.9
3	21	triethylamine	67.6
4	21	water	73.5

<sup>a</sup>Experimental conditions: flow rate of DMAOL (3.8 wt % in methanol) solution: 0.5 mL/min;  $T = 313.15$  K;  $F_G = 40$  sccm (the molar ratio of  $H_2$  to DMAOL: 26); the amount of the 7 wt %  $Pd(OH)_2/Al_2O_3$  catalyst (diluted with 4.0 g alumina sphere): 1.0 g; and the concentration of additive is 8.8 wt % in entry 2, 3, and 4.

It is found that the conversion of entry 2 is higher than that of entry 1 while the conversion of entry 3 is lower than that of entry 1. The results indicate that acidic conditions favor the removal of the diphenylmethyl group, while basic conditions inhibit the removal of the diphenylmethyl group. The results indicate that debenzylation with hydrogenolysis can be enhanced by addition of acetic acid into the solution and the addition of basic additive should be avoided. The conversions of entry 4 is also slightly lower, indicating that the existence of water would have an adverse effect on the reaction. The exact reason for the adverse effect of water on the reaction is still unclear, which required further investigation.

**Reaction Performance Test.** In this part, we compared the reaction performance of a traditional batch reactor (250 mL volume) with that of the micropacked-bed reactor. Here, the mass of the substrate converted per unit time of the unit reactor volume [ $g(\text{raw material}) \times mL(\text{reactor volume})^{-1} \times \text{min}^{-1}$ ] was used to evaluate the reactor performance. As shown in Table 3, the reaction rate in the batch reactor was

**Table 3. Comparison of Performances of Traditional Batch and Micropacked-Bed Reactors<sup>a</sup>**

entry	residence time	conversion/%	reactor performance [ $g(\text{raw material}) \times mL(\text{reactor volume})^{-1} \times \text{min}^{-1}$ ]
1	3.0 h	18.5	$2.5 \times 10^{-5}$
2	5.0 h	38.1	$3.1 \times 10^{-5}$
3	1.9 min	63.0	$3.1 \times 10^{-3}$

<sup>a</sup>Experimental conditions: initial concentration of DMAOL in methanol: 3.8 wt %;  $T = 333.15$  K;  $P = 21$  bar; the amount of the  $Pd(OH)_2/Al_2O_3$  catalyst (7 wt %): 0.5 g; entry 1 and 2 were carried out in traditional batch: stirring speed was 200 rpm to avoid the damage of catalysts; raw material volume was 200 mL; and entry 3 was carried out in a micropacked-bed reactor:  $F_L = 0.5$  mL/min,  $F_G = 40$  sccm (the molar ratio of  $H_2$  to DMAOL: 26).

very slow with a low conversion of 18.5% after 3 h and 38.1% after 5 h. The main reason is the limited gas–liquid mass transfer rate in the batch reactor. In contrast, because of the larger interfacial area and shorter diffusion distance in micropacked reactors, a high conversion of 63% can be obtained with only a short residence time of 1.9 min. In addition, the value of conversion per unit volume per unit time of the micropacked-bed reactor is 100 times that of the batch.

As a result, the micropacked-bed reactor is more efficient for the hydrogenation of DMAOL than the traditional batch reactor.

To further study the long-term stability of the reaction system and catalyst life of  $Pd(OH)_2/Al_2O_3$ , the reaction performance was investigated in the micropacked-bed reactor for 240 h as shown in Figure 4. In order to achieve the

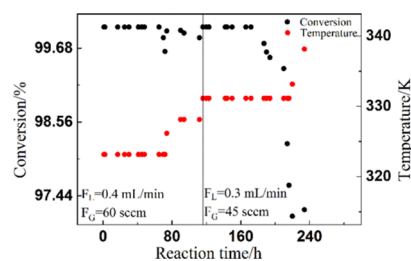


**Figure 4.** Stability of the reaction system in the micropacked-bed reactor. Experimental conditions: initial concentration of 1-(diphenylmethyl)-3-hydroxyazetidine: 10 wt %;  $P = 25$  bar; and the amount of the  $Pd(OH)_2/Al_2O_3$  catalyst (7 wt %): 4.3 g. When the reaction time is less than 116 h,  $F_L = 0.4$  mL/min,  $F_G = 60$  sccm; when the reaction time is more than 116 h,  $F_L = 0.3$  mL/min,  $F_G = 45$  sccm.

maximum reaction conversion, the catalyst bed was not diluted with alumina sphere fillers (4.3 g  $Pd(OH)_2/Al_2O_3$ ) and the concentration of the substrate was further improved to 10 wt % in this experiment. As first, the fresh catalyst had a high catalytic activity and the conversion could reach 100% for 70 h. After 70 h, the conversion began to decrease because of the deactivation of the catalyst. The reason of deactivation and the following regeneration method are still unclear and we are still working on them. The most possible reason for the deactivation is the adsorption of substances on the precise metal catalyst because of the strong interaction between amine and the precise metal. To increase the reaction rate, the reaction temperature was gradually increased to maintain the high conversion. After 116 h, the liquid flow rate was decreased from 0.4 to 0.3 mL/min to increase the residence time to ensure the conversion. By increasing the temperature and decreasing the flow rate, the conversion of the substrate could stay above 99.5% for 190 h. After that, the conversion decreased rapidly indicating that a severe catalyst deactivation occurred and the catalyst was required to be replaced or regenerated. From the results in Figure 4, it demonstrates that about 90 g DMAOL can be efficiently converted to the product for 1 g  $Pd(OH)_2/Al_2O_3$  catalyst in the micropacked bed and the continuous flow system can achieve an efficient production of 3-azetidinol for 190 h (the temperature and liquid flow rate were changed after 70 h). However, more issues such as heat transfer, gas–liquid mixing, and pressure drop across the packed bed should be carefully considered in the scaling up of this continuous system.

**Kinetics Study of Hydrogenolysis of DMAOL. Mass Transfer Considerations.** In a three-phase catalytic reaction system, the mass transfer typically includes three steps in series: dissolution of  $H_2$  in liquid, diffusion of dissolved  $H_2$  through liquid to the solid catalyst surface, and intraparticle diffusion to the active catalytic sites, which can influence the reaction kinetics.<sup>23</sup> Therefore, it is important to confirm that the mass transfer limitation can be ignored before determining the kinetic parameters.

First, external mass transfer should be carefully evaluated.<sup>10a</sup> Because of the use of pure hydrogen as a reactant, the mass transfer resistance occurring in the gas film side of the gas–liquid interface can be ignored, and the mass transfer resistance on the liquid side at the gas–liquid interface and the mass transfer resistance at the liquid–solid interface should be considered.<sup>24</sup> Exploring the effect of different liquid superficial velocities (flow rate/cross-sectional area of the packed bed) on the reaction rate at the same residence time can be used to determine whether the external mass transfer limitation can be ignored.

In the present study, four  $\mu$ PBRs with the same volume (3.0 mL) and different internal diameters (4.35; 4.57; 5.35; and 5.75 mm) were designed for the experiments. These reactors were filled with the same amount of the catalyst. This method can successfully achieve different liquid superficial velocities in different reactors under the same flow rate and residence time.

Figure 5 shows that when the liquid superficial velocity exceeds 5.0 cm/min, the average reaction rate does not change

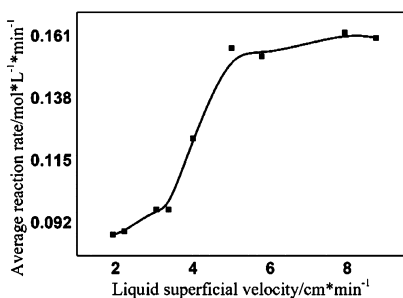


**Figure 5.** Effect of different liquid superficial velocities on the average reaction rate. Experimental conditions: initial concentration of DMAOL: 5.7 wt %;  $P = 21$  bar;  $T = 313.15$  K;  $F_G = 40$  sccm; and the amount of the 7 wt % Pd(OH)<sub>2</sub>/Al<sub>2</sub>O<sub>3</sub> catalyst (diluted with 4.0 g alumina sphere): 1.0 g.

significantly as the liquid velocity increases. This result indicates that the reaction is independent of external mass transfer when the liquid superficial velocity is greater than 5.0 cm/min. It can be considered that the external mass transfer resistance has been eliminated.

Internal mass transfer limitations within the porous media were evaluated by calculating the Weisz modulus ( $M_w$ ), which ratios the effective reaction time and the diffusion time within the catalyst particle.<sup>25</sup> The Weisz modulus of the substrate and H<sub>2</sub> were calculated as shown in the Supporting Information. The values of the Weisz modulus were determined to be 0.123 and 0.776, for H<sub>2</sub> and DMAOL, respectively, indicating only minor contributions from intraparticle diffusion and the internal mass transfer resistance can be ignored.

**Kinetic Model of Hydrogenolysis of DMAOL.** The reaction kinetic model was studied after the internal and external transfer resistances were eliminated to ensure that the reaction was in the kinetic-control region. Here, the kinetics is presented by a power-law model, which can be described by an empirical kinetic expression

$$r = k' C_A^\alpha P^\beta = -\frac{dC_A}{dt} \quad (3)$$

where  $\alpha$  and  $\beta$  are the reaction orders of reactants.

First, the value of  $\alpha$  was determined by changing the initial concentration of the reactants at the same residence time.

During the experiment, it was found that there was no significant pressure drop in the reactor through the pressure gauges at the inlet and outlet of the packed bed reactor, the reaction pressure can be considered to be constant. At first, the temperature and pressure were kept unchanged, the term  $k'P^\beta$  could be regarded as a constant  $K$ , and the following equation is obtained

$$r = KC_A^\alpha = -\frac{dC_A}{dt} \quad (4)$$

After integrating eq 4 and considering the boundary conditions [ $t = 0$ ,  $C_A = C_{A0}$ ;  $t = \tau$ ,  $C_A = C_{A0}(1 - X)$ ], eq 5 is obtained.

$$X = 1 - \left[ \frac{K\tau(\alpha - 1)}{C_{A0}^{1-\alpha}} + 1 \right]^{1/1-\alpha} \quad (5)$$

The hydrogenolysis of DMAOL was performed at nine initial concentrations ranging from 0.033 to 0.33 mol/L and the conversions at different concentrations are given in Figure 6. The experimental data was fitted with eq 5. It was found that

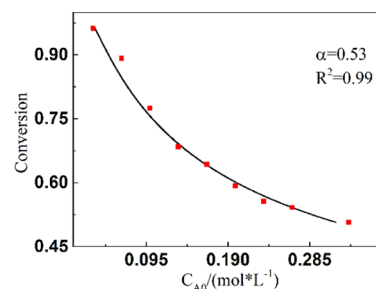


**Figure 6.** Conversion vs the initial concentration of DMAOL in methanol. Experimental conditions:  $P = 21$  bar;  $T = 313.15$  K;  $F_G = 40$  sccm;  $F_L = 0.9$  mL/min;  $\tau = 63.6$  s; and the amount of the 7 wt % Pd(OH)<sub>2</sub>/Al<sub>2</sub>O<sub>3</sub> catalyst (diluted with 4.0 g alumina sphere): 1.0 g.

when  $\alpha$  is 0.53, the calculated curve agreed well with the experimental values ( $R^2 = 0.99$ ), indicating that the reaction order of DMAOL is 0.53.

The value of  $\beta$  is determined by changing the reaction pressure at the same residence time. The liquid holdup is related to the superficial velocities of the gas and liquid. The change of the reaction pressure will lead to an obvious change for the superficial velocity of the gas and corresponding residence time of liquid. To eliminate the effect of reaction pressure on the residence time, the liquid flowrate was varied from 0.58 to 1.04 mL/min according to the model described in the literature<sup>16</sup> to ensure the same residence time. Taking  $\alpha = 0.53$ , integrating and deforming eq 3, eq 6 was obtained.

$$X = 1 - \left[ 1 - \frac{0.47k'\tau P^\beta}{C_{A0}^{0.47}} \right]^{1/0.47} \quad (6)$$

The hydrogenolysis of DMAOL was performed at nine reaction pressures and the obtained experimental results are shown in Figure 7. Then the experimental data was fitted with eq 6. It shows that when  $\beta$  is 0.31, the calculated curve agreed well with the experimental values ( $R^2 = 0.97$ ), indicating that the reaction order of hydrogen pressure is 0.31.

After determining the values of  $\alpha$  and  $\beta$ , the two values substituted into eqs 3, 7 can be obtained to calculate the value of  $k'$ .

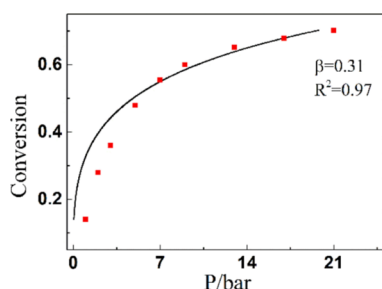


**Figure 7.** Conversion vs the reaction pressure. Experimental conditions:  $C_{A0} = 0.20$  mol/L;  $T = 313.15$  K;  $F_G = 40$  sccm; flow velocity = 16.32 cm/min;  $\tau = 73.5$  s; and the amount of the 7 wt % Pd(OH)<sub>2</sub>/Al<sub>2</sub>O<sub>3</sub> catalyst (diluted with 4.0 g alumina sphere): 1.0 g.

$$k' = \frac{C_{A0}^{0.47} [1 - (1 - X)^{0.47}]}{0.47 P^{0.31} \tau} \quad (7)$$

Figure 8a shows the conversions at varied reaction temperatures ranging from 303.15 to 343.15 K. The results

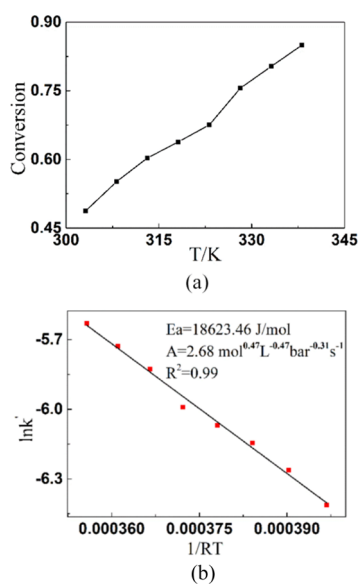


**Figure 8.** (a) Conversion vs the reaction temperatures. (b) Plot of  $\ln k'$  vs  $1/RT$ . Experimental conditions:  $C_{A0} = 0.20$  mol/L;  $P = 21$  bar;  $F_G = 40$  sccm;  $F_L = 0.9$  mL/min;  $\tau = 63.6$  s; and the amount of the Pd(OH)<sub>2</sub>/Al<sub>2</sub>O<sub>3</sub> catalyst (7 wt %): 1.0 g.

indicate that the reaction rate increases as the temperature increases. The values of  $k'$  at different temperatures were calculated with eq 7. According to the Arrhenius formula,  $k' = Ae^{-E_a/RT}$ , the activation energies ( $E_a$ ) and Arrhenius constant ( $A$ ) can be obtained by fitting  $\ln k'$  and  $1/RT$  as shown in Figure 8b, which are  $18.6 \pm 0.7$  kJ/mol and  $2.68 \pm 0.25$  mol<sup>0.47</sup>/(L<sup>0.47</sup>·bar<sup>0.31</sup>·s), respectively ( $R^2 = 0.99$ ).

After all the parameters were obtained, the kinetic model could be established.

$$r = 2.68 \left( \frac{\text{mol}^{0.47}}{L^{0.47} \cdot \text{bar}^{0.31} \cdot \text{s} \cdot \text{gcat}} \right) \times e^{-1.86 \times 10^4 (\text{J/mol}) / 8.314 (\text{J} \cdot \text{mol}^{-1} \cdot \text{K}^{-1}) \times T} C_A^{0.53} P^{0.31} \quad (8)$$

The type of adsorption of the reactant on the catalyst and the rate-determining step of the reaction were studied after the

kinetic model was established. The heterogeneous hydrogenation rate is determined by one of the steps of adsorption of the substrate or hydrogen, desorption of the product, and surface reaction when the reaction is in the kinetics-control zone.<sup>26</sup> In addition, because of the different adsorption mechanisms of the reactants on the porous catalysts, research work on kinetic models has been further complicated. Based on the Langmuir equation, many rate expressions were studied in this paper.

Because of the different adsorption mechanisms of the reactants,<sup>26</sup> there are up to 16 different theoretical kinetic models. All the possible theoretical models have been fitted with the experimental data. If a mathematical model agrees well with the data, the model can be considered to be the reaction kinetic model.

After excluding the other 15 models, the kinetic model was obtained ( $R^2 = 0.99$  for  $C_{A0}$ ,  $R^2 = 0.96$  for  $P$ , the detailed process and fitting results are shown in Supporting Information)

$$r = \frac{k K_A C_A K_H P}{(1 + K_A C_A + K_B C_B)(1 + \sqrt{K_H P})^2} \quad (9)$$

where,  $k$ ,  $K_A$ ,  $K_B$ , and  $K_H$  are the reaction rate constant, adsorption equilibrium constant of substrate, product, and H<sub>2</sub>, respectively.

Based on the kinetic model, we can find that the diphenylmethyl removal rate of DMAOL with the Pd(OH)<sub>2</sub>/Al<sub>2</sub>O<sub>3</sub> catalyst was controlled by the surface reaction rate, and the adsorption type of the substrate and H<sub>2</sub> on the catalyst are noncompetitive and dissociative adsorption. Hwang<sup>22b</sup> et al. studied the debenzilation of *N*-benzyl-4-fluoroaniline, and the obtained rate-determining step and the adsorption type of the reactant on the catalyst were consistent with the conclusions in our study. In addition, compared with the activation energy value (138.4 kJ/mol) obtained by Hwang, we found that the activation energy value (18.6 kJ/mol) in our study is very small, which indicate that the palladium hydroxide catalyst have better catalytic activity for debenzilation than the palladium catalyst. The kinetic model obtained in this study may be helpful for the reactor design and process optimization for the continuous deprotection development.

## CONCLUSIONS

In this study, a micropacked-bed reactor has been successfully applied to the continuous hydrogenation of DMAOL using hydrogen gas. It is demonstrated that the  $\mu$ PBRs are more efficient for the hydrogenation of DMAOL than the traditional batch reactor. The conversion per unit reactor volume per unit time in the micropacked-bed reactor is 100 times that of the batch. The reaction kinetics model was obtained after the external and internal mass transfer limitations have been eliminated and the reaction is in the kinetics-control region. The reaction rate is found to be 0.53 order with respect to DMAOL concentration and 0.31 order to hydrogen pressure. The activation energy ( $E_a$ ) of the rate constant is 18.6 kJ/mol and the Arrhenius constant ( $A$ ) is  $2.68$  mol<sup>0.47</sup>/(L<sup>0.47</sup>·bar<sup>0.31</sup>·s). The experimental results were fitted with several kinetic models to determine the rate-determining step, which indicated that the diphenylmethyl removal rate of DMAOL with the Pd(OH)<sub>2</sub>/Al<sub>2</sub>O<sub>3</sub> catalyst was controlled by the surface reaction rate, and the adsorption type of the substrate and H<sub>2</sub> on the catalyst are noncompetitive and dissociative adsorption.



## ■ ASSOCIATED CONTENT

### Supporting Information

The Supporting Information is available free of charge at <https://pubs.acs.org/doi/10.1021/acs.oprd.9b00416>.

Calculation of the Weisz modulus and detailed results on the intrinsic kinetic model fitting (PDF)

## ■ AUTHOR INFORMATION

### Corresponding Author

\*E-mail: [jszhang@tsinghua.edu.cn](mailto:jszhang@tsinghua.edu.cn).

### ORCID

Jisong Zhang: 0000-0002-4925-7355

### Notes

The authors declare no competing financial interest.

## ■ ACKNOWLEDGMENTS

We gratefully acknowledge the supports of the National Natural Science Foundation of China (21978146), Tsinghua University Initiative Scientific Research Program (2019Z08QCX02), and the State Key Laboratory of Chemical Engineering (SKL-ChE-17T01) on this work.

## ■ NOMENCLATURE

$F_L$	liquid flow rate, mL/min
$F_G$	gas flow rate, sccm
$P$	pressure, bar
$T$	temperature, K
$h$	liquid holdup, –
$D$	reactor inner diameter, cm
$L$	reactor length, cm
$C_A$	concentration of DMAOL, mol/L
$C_B$	concentration of diphenylmethane, mol/L
$C_{A0}$	initial concentration of DMAOL, mol/L
$X$	conversion of <i>N</i> -diphenylmethylazetidin-3-ol, m/s <sup>2</sup>
$E_a$	activation energy, kJ/mol
$A$	Arrhenius constant, mol <sup>0.47</sup> /L <sup>0.47</sup> ·bar <sup>0.31</sup> ·s·gcat

### Greek letters

$\tau$	liquid residence time, s
$\epsilon$	porosity, –

### Subscripts

G	gas
L	liquid

## ■ REFERENCES

- (1) Carey, J. S.; Laffan, D.; Thomson, C.; Williams, M. T. Analysis of the reactions used for the preparation of drug candidate molecules. *Org. Biomol. Chem.* **2006**, *4*, 2337–2347.
- (2) Sartori, G.; Ballini, R.; Bigi, F.; Bosica, G.; Maggi, R.; Righi, P. Protection (and deprotection) of functional groups in organic synthesis by heterogeneous catalysis. *Chem. Rev.* **2004**, *104*, 199–250.
- (3) (a) Albano, G.; Evangelisti, C.; Aronica, L. A. Hydrogenolysis of Benzyl Protected Phenols and Aniline Promoted by Supported Palladium Nanoparticles. *ChemistrySelect* **2017**, *2*, 384–388. (b) Ishihara, K.; Hiraiwa, Y.; Yamamoto, H. Homogeneous debenzoylation using extremely active catalysts: Tris (triflyl) methane, scandium (III) tris (triflyl) methide, and copper (II) tris (triflyl) methide. *Synlett* **2000**, *2000*, 80–82.
- (4) Olah, G. A.; Kobayashi, S.; Tashiro, M. Aromatic substitution. XXX. Friedel-Crafts benzylation of benzene and toluene with benzyl and substituted benzyl halides. *J. Am. Chem. Soc.* **1972**, *94*, 7448–7461.

(5) Tsuchimoto, T.; Hiyama, T.; Fukuzawa, S.-i. Scandium(III) trifluoromethanesulfonate-catalysed reductive Friedel-Crafts benzylation of aromatic compounds using arenecarbaldehydes and propane-1,3-diol. *Chem. Commun.* **1996**, 2345–2346.

(6) (a) Mao, J.; Gregory, D. Recent advances in the use of sodium borohydride as a solid state hydrogen store. *Energies* **2015**, *8*, 430–453. (b) Watanabe, T.; Kobayashi, A.; Nishiura, M.; Takahashi, H.; Usui, T.; Kamiyama, I.; Mochizuki, N.; Noritake, K.; Yokoyama, Y.; Murakami, Y. Synthetic Studies on Indoles and Related Compounds. XXVI. The Debenzylation of Protected Indole Nitrogen with Aluminum Chloride. (2). *Chem. Pharm. Bull.* **1991**, *39*, 1152–1156. (c) Rombouts, F.; Franken, D.; Martínez-Lamenca, C.; Braeken, M.; Zavattaro, C.; Chen, J.; Trabanco, A. A. Microwave-assisted *N*-debenzylation of amides with triflic acid. *Tetrahedron Lett.* **2010**, *51*, 4815–4818.

(7) Rogers, L.; Jensen, K. F. Continuous manufacturing—the Green Chemistry promise? *Green Chem.* **2019**, *21*, 3481.

(8) Beeck, O. Hydrogenation catalysts. *Discuss. Faraday Soc.* **1950**, *8*, 118–128.

(9) Yoswathananont, N.; Nitta, K.; Nishiuchi, Y.; Sato, M. Continuous hydrogenation reactions in a tube reactor packed with Pd/C. *Chem. Commun.* **2005**, *1*, 40–42.

(10) (a) Wiles, C.; Watts, P. Continuous flow reactors: a perspective. *Green Chem.* **2012**, *14*, 38–54. (b) Jiménez-González, C.; Poehlauer, P.; Broxterman, Q. B.; Yang, B.-S.; Am Ende, D.; Baird, J.; Bertsch, C.; Hannah, R. E.; Dell'Orco, P.; Noorman, H.; Yee, S.; Reintjens, R.; Wells, A.; Massonneau, V.; Manley, J. Key green engineering research areas for sustainable manufacturing: a perspective from pharmaceutical and fine chemicals manufacturers. *Org. Process Res. Dev.* **2011**, *15*, 900–911.

(11) (a) Calabrese, G. S.; Pissavini, S. From batch to continuous flow processing in chemicals manufacturing. *AIChE J.* **2011**, *57*, 828–834. (b) Jensen, K. F. Flow chemistry—Microreaction technology comes of age. *AIChE J.* **2017**, *63*, 858–869. (c) Britton, J.; Raston, C. L. Multi-step continuous-flow synthesis. *Chem. Soc. Rev.* **2017**, *46*, 1250–1271. (d) Cantillo, D.; Kappe, C. O. Halogenation of organic compounds using continuous flow and microreactor technology. *React. Chem. Eng.* **2017**, *2*, 7–19.

(12) Losey, M. W.; Schmidt, M. A.; Jensen, K. F. Microfabricated multiphase packed-bed reactors: characterization of mass transfer and reactions. *Ind. Eng. Chem. Res.* **2001**, *40*, 2555–2562.

(13) Desai, B.; Dallinger, D.; Kappe, C. O. Microwave-assisted solution phase synthesis of dihydropyrimidine C5 amides and esters. *Tetrahedron* **2006**, *62*, 4651–4664.

(14) Matos, M.-C.; Murphy, P. V. Synthesis of Macrolide–Saccharide Hybrids by Ring-Closing Metathesis of Precursors Derived from Glycolols and Benzoic Acids. *J. Org. Chem.* **2007**, *72*, 1803–1806.

(15) (a) Anthoni, U.; Nielsen, P. H.; Smith-Hansen, L.; Wium-Andersen, S.; Christophersen, C. Charamin, a quaternary ammonium ion antibiotic from the green alga *Chara globularis*. *J. Org. Chem.* **1987**, *52*, 694–695. (b) Huang, X.; Bao, Y.; Zhu, S.; Zhang, X.; Lan, S.; Wang, T. Synthesis and biological evaluation of levofloxacin core-based derivatives with potent antibacterial activity against resistant Gram-positive pathogens. *Bioorg. Med. Chem. Lett.* **2015**, *25*, 3928–3932.

(16) Zhang, J.; Teixeira, A. R.; Kögl, L. T.; Yang, L.; Jensen, K. F. Hydrodynamics of gas-liquid flow in micropacked beds: Pressure drop, liquid holdup, and two-phase model. *AIChE J.* **2017**, *63*, 4694–4704.

(17) David, A.; Vannice, M. Control of catalytic debenzoylation and dehalogenation reactions during liquid-phase reduction by H<sub>2</sub>. *J. Catal.* **2006**, *237*, 349–358.

(18) Pearlman, W. M. Noble metal hydroxides on carbon nonpyrophoric dry catalysts. *Tetrahedron Lett.* **1967**, *8*, 1663–1664.

(19) (a) Bernotas, R. C.; Cube, R. V. The Use of Pearlman's Catalyst for Selective *N*-Debenzylation in the Presence of Benzyl Ethers. *Synth. Commun.* **1990**, *20*, 1209–1212. (b) Bellamy, A. J. Reductive

debenzylation of hexabenzylhexaazaisowurtzitane. *Tetrahedron* **1995**, *51*, 4711–4722.

(20) (a) Studer, M.; Blaser, H.-U. Influence of catalyst type, solvent, acid and base on the selectivity and rate in the catalytic debenzylation of 4-chloro-N,N-dibenzyl aniline with Pd/C and H<sub>2</sub>. *J. Mol. Catal. A: Chem.* **1996**, *112*, 437–445. (b) Chen, J.; Thakur, D. S.; Wiese, A. F.; White, G. T.; Penquite, C. R. *Preparation and Characterization of High Activity and Low Palladium-Containing Debenzylation Catalysts*; Chemical Industries-New York-Marcel Dekker, 2003; pp 313–328.

(21) Fajt, V.; Kurc, L.; Červený, L. The effect of solvents on the rate of catalytic hydrogenation of 6-ethyl-1,2,3,4-tetrahydroanthracene-9,10-dione. *Int. J. Chem. Kinet.* **2008**, *40*, 240–252.

(22) (a) Schelhaas, M.; Waldmann, H. Protecting group strategies in organic synthesis. *Angew. Chem., Int. Ed. Engl.* **1996**, *35*, 2056–2083.

(b) Hwang, H. T.; Martinelli, J. R.; Gounder, R.; Varma, A. Kinetic study of Pd-catalyzed hydrogenation of N-benzyl-4-fluoroaniline. *Chem. Eng. J.* **2016**, *288*, 758–769. (c) Sajiki, H.; Kuno, H.; Hirota, K. Suppression effect of the Pd/C-catalyzed hydrogenolysis of a phenolic benzyl protective group by the addition of nitrogen-containing bases. *Tetrahedron Lett.* **1998**, *39*, 7127–7130.

(23) (a) Yang, C.; Teixeira, A. R.; Shi, Y.; Born, S. C.; Lin, H.; Li Song, Y.; Martin, B.; Schenkel, B.; Peer Lachegurabi, M.; Jensen, K. F. Catalytic hydrogenation of N-4-nitrophenyl nicotinamide in a micro-packed bed reactor. *Green Chem.* **2018**, *20*, 886–893. (b) Ramachandran, P.; Chaudhari, R. *Three-Phase Catalytic Reactors*; Gordon & Breach Science Pub, 1983; Vol. 2.

(24) Ye, X.; An, Y.; Xu, G. Kinetics of 9-ethylcarbazole hydrogenation over Raney-Ni catalyst for hydrogen storage. *J. Alloys Compd.* **2011**, *509*, 152–156.

(25) Poling, B. E.; Prausnitz, J. M.; O'Connell, J. P. *The Properties of Gases and Liquids*; McGraw-hill: New York, 2001; Vol. 5.

(26) Bao-jun, L. M. C.; Xiao-mu, X. Constitution of Dynamics Equation for Heterogeneous Catalytic Hydrogenation. *J. Chem. Adhes.*, **2005**, *2*, DOI: 10.3969/j.issn.1001-0017.2005.02.009.